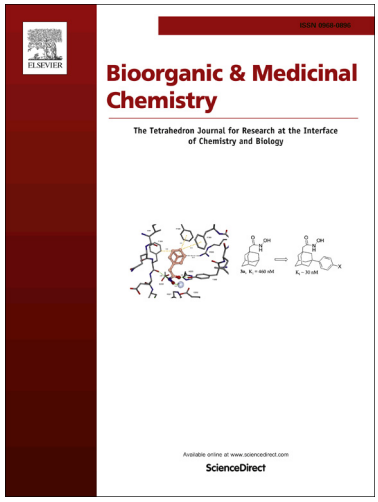

Identification of novel inhibitors of Aurora A with a 3-(pyrrolopyridin-2-yl)indazole scaffold

Pinrao Song, Ming Chen, Xiaodong Ma, Lei Xu, Tao Liu, Yubo Zhou, Yongzhou Hu

PII: S0968-0896(15)00088-7
DOI: http://dx.doi.org/10.1016/j.bmc.2015.02.004
Reference: BMC 12067

To appear in: *Bioorganic & Medicinal Chemistry*

Received Date: 20 November 2014
Revised Date: 3 February 2015
Accepted Date: 5 February 2015

Please cite this article as: Song, P., Chen, M., Ma, X., Xu, L., Liu, T., Zhou, Y., Hu, Y., Identification of novel inhibitors of Aurora A with a 3-(pyrrolopyridin-2-yl)indazole scaffold, *Bioorganic & Medicinal Chemistry* (2015), doi: http://dx.doi.org/10.1016/j.bmc.2015.02.004

Identification of novel inhibitors of Aurora A with a 3-(pyrrolopyridin-2-yl)indazole scaffold

Pinrao Song[a], Ming Chen[a], Xiaodong Ma[a], Lei Xu[b], Tao Liu[a,*], Yubo Zhou[b,*], Yongzhou Hu[a,*]

[a] *ZJU-ENS Joint Laboratory of Medicinal Chemistry, Zhejiang Province Key Laboratory of Anti-Cancer Drug Research, College of Pharmaceutical Sciences, Zhejiang University, Hangzhou 310058, China*

[b] *National Center for Drug Screening, State Key Laboratory of Drug Research, Shanghai Institute of Materia Medica, Chinese Academy of Sciences, Shanghai 201203, China*

Abstract: A novel series of 3-(pyrrolopyridin-2-yl)indazole derivatives were synthesized and biologically evaluated for their anti-proliferative effects on five human cancer cell lines. As a result, all of them exhibited vigorous potency against HL60 cell line with IC_{50} values ranging from singe digital nanomolar to micromolar level. Besides, a majority of them displayed modest to good antiproliferative activities against the other four cell lines, including KB, SMMC-7721, HCT116, and A549. Particularly, compound **2y**, as the most distinguished one in this series, demonstrated IC_{50} values of 8.3 nM and 1.3 nM against HL60 and HCT116 cell lines, respectively. Afterwards, for exploring the molecular target, compounds **2d**, **2g** and **2y** were further selected to evaluate the inhibitory activities against a panel of kinases. Finally, they were identified to be targeting Aurora A kinase with significant selectivity over other kinases, such as CHK1, CDK2, MEK1, GSK3β, BRAF, IKKβ and PKC.

Keywords: Pyrrolopyridin-indazoles; Antiproliferative agents; Cell cycle profile; Aurora A inhibitors; Selectivity

*Corresponding author:
Tao Liu, Tel: +86-571-88208458; Fax: +86-571-88981051; *E-mail address:* lt601@zju.edu.cn
Yubo Zhou, Tel: +86-21-5080-1313; Fax: +86-21-5080-1313; *E-mail address:* ybzhou@mail.shcnc.ac.cn
Yongzhou Hu, Tel/Fax: +86-571-8820-8460; *E-mail address:* huyz@zju.edu.cn

1. Introduction

Cellular proliferation and growth, as a set of timely ordered events, are governed by a plethora of protein kinases. Among them, checkpoint kinases (CHKs), cyclin-dependent kinases (CDKs), aurora kinases (AURKs) and polo-like kinases (PLKs), play an essential role in the cell cycle progression.[1] Phosphorylation or dephosphorylation of these functional proteins may be viewed as molecular on/off switches involved in many distinct cellular processes, such as proliferation, differentiation, transcription, translation, and apoptosis.[2] On the other hand, the frequent mutation or overexpression of these kinases has been observed in a broad range of human malignancies, thereby providing a unique opportunity for anti-cancer intervention.[3] As validated by ample experimental results, inhibition of these functional proteins would result in cell accumulation at certain phases (G1, S, or G2/M) and induce apoptosis of tumor cells.[4] Currently, quite a number of small-molecule inhibitors targeting cell cycle kinases have been developed and advanced into clinical trials.[5] However, their further development as chemotherapeutic drugs has been compromised due to lack of long term efficacy and severe side effects caused by low selectivity over normal proliferating cells. Hence, there is presently an urgent demand of more drug-like small-molecule inhibitors with novel and distinct chemotypes.

Our group has been continuously devoted to the synthesis and biological evaluations of small molecule heterocyclic compounds and has established an in-house compound library. As a part of our recent work, a novel structural series of 5-amide pyrrolopyridin-indazoles have been prepared. During our speculation of their potential biological activities, we were attracted by their structural similarity to a novel chemical entity **1** that targeting cell cycle. Discovered by Merck Research Laboratories, this 5-substituted indole-indazole derivative exhibited IC_{50} values of 30 nM and 11 nM against CHK1 and CDK7, respectively (Fig. **1**). The indole-indazole scaffold of **1** provided a hydrogen bond donor-acceptor-donor motif, through which contacts to the hinge backbones of the ATP-binding sites of numerous protein kinases could be captured.[6] The pyrrolopyridin-indazole moiety in our compounds could be viewed as a bioisostere of the indole-indazole core, which may represent a novel and distinct template for the exploration of chemotherapeutic antitumor agents. Meanwhile, the pyrrolopyridin-indazole core may mimic the indole-indazole as the hinge binder to develop kinase inhibitors. With such a 5-amide pyrrolopyridin-indazole scaffold in hand, our medicinal chemistry effort was geared towards variation of the substitutions on the C5-amide linker with a variety of aromatic or alkyl groups to explore the antiproliferative effect. Besides, sulfamide and urea were also investigated as surrogates for the amide linker. Of greater gratification was that derivative **2y** bearing a urea linker displayed antiproliferative activity in the low nanomolar range and induced G2/M cell cycle arrest in the cell cycle profile (FACS) analysis. In a biochemical assay, the representative compounds **2d**, **2g** and **2y**, showed great specificity for Aurora A inhibition and little inhibition against other kinases being tested. Moreover, the binding modes of **2d** and **2y** bound to Aurora A kinase were interpreted using in silico docking experiments.

< Insert Fig. **1**>

2. Results and discussion

2.1. Chemistry

The general synthetic route of these 5-substituted pyrrolopyridin-indazole derivatives are illustrated in Schemes **1**-**3**. The intermediates indazoles **7a-c** and 4-azaindole **14** were prepared

following the method described in the literature with minor modifications.[5] Starting from the commercial available 2-methylanilines **3a-c**, the 1*H*-indazoles **4a-c** were obtained via diazotization using $NaBF_4/NaNO_2$ and followed by an *in-situ* intramolecular cyclization. After substitution of **4a-c** with I_2 in the presence of KOH, the newly formed **5a-c** were coped with ethylmagnesium bromide and chlorotributyltin to afford **6a-c**. Subsequently, *N*-Boc protection was carried out to afford intermediates **7a-c**.

Meanwhile, the commercially available **8** was subjected to nitration with a mixture of concentrated HNO_3 and H_2SO_4, which furnished **9** as the product. Afterwards, its amine was masked with Boc-protecting group and then methylated with methyl iodide to afford **11**. Via condensation with DMFDMA, the generated intermediate underwent a one pot catalytic hydrogenation and cyclization to produce **12**. At the next step, the iodide fragment **14** was achieved by treatment of Boc-protected product **13** with I_2 in the presence of n-butyllithium.

With **7a-c** and **14** in hand, critical intermediates **15a-c** were prepared from **7a-c** and **14** through a classical Stille coupling reaction. Subsequent removal of all the Boc-protecting groups under acidic conditions gave the intermediates **16a-c**. Finally, the secondary amines were converted into amides, sulfonamides or ureas via reacting with corresponding acid chlorides, sulfonyl chlorides or isocyanates to afford the target compounds **2a-n**, **2o-x**, and **2y-z**, respectively.

< Insert Scheme **1**>

< Insert Scheme **2**>

< Insert Scheme **3**>

2.2. Tumor cell growth inhibition studies

All the above compounds were tested for their antiproliferative activities in vitro against five human cancer cell lines (HL60, KB, SMMC-7721, HCT116, and A549) with MTT assay via introducing Taxol as a positive control.

As illustrated in Table **1** and **2**, it is clear that most of the compounds bearing an amide or sulfamide linkage were more effective against HL60 cell line than against the other four cell lines with IC_{50} values at the submicromolar or low micromolar level (HL60: IC_{50} = 0.45-6.80 μM) except for the compounds bearing a urea linkage (**2y** and **2z**). Incorporation of halogen functionalities on the 4-position of the phenyl ring slightly enhanced the potency, as exemplified by compounds **2f-h**, which were over 3-fold more potent relative to the unsubstituted counterpart **2d**. Among them, **2g** bearing a chlorine substituent was the most cytotoxic compound with IC_{50} values of 0.45 μM and 0.63 μM against HL60 and KB cell lines, respectively. Introduction of electron-donating methoxyl group (**2i** and

2j), electron-withdrawing nitro group (**2k**) or replacement of the phenyl ring with a furan moiety (**2l**), despite retention of cytotoxicity against HL60 cell line, led to a decrease in efficacy against the other four cell lines. Besides, a slight loss in antiproliferative activities was observed when replacing the benzene ring with alkyl groups (**2a-c** versus **2d**). The chlorine atom at the 6-position of the indazole ring was tolerable since the analog **2m** displayed little differentiation in cytotoxic activity compared to **2d**, whereas introduction of a cyano group (**2n**) caused a dramatic loss of potency against KB, SMMC-7721, HCT116, and A549, except for HL60. Similarly, derivatives **2o** and **2q-s** with a common tertiary sulfamide linker exhibited comparable activities to their amide counterparts **2d** and **2g-i**. It is noteworthy that compounds **2y** and **2z** with a urea linker stood out as the most potent compounds with nanomolar IC_{50} values against HL60 and HCT116 cell lines, respectively. Particularly, derivative **2y** with an inhibitory IC_{50} value of 1.3 nM against HCT116 cell line, was found to be 3-fold more efficient than the well-known cytotoxic agent Taxol.

< Insert Table **1**>

< Insert Table **2**>

2.3. Cell cycle profile (FACS) analysis

By virtue of its distinguished antiproliferative activities, compound **2y** was further evaluated for its effects on the cell cycle by flow cytometry using HCT116 cells (Fig. **2**). Our results demonstrated that treatment of HCT116 cells with **2y** at 50, 100 and 200 nM for 24 h induced G2/M cell cycle arrest in a concentration-dependent manner. At concentration up to 100 nM, compound **2y** caused significant alteration of cell distribution relative to the DMSO control. Treatment with **2y** at a higher concentration of 200 nM led to a remarkable arrest at G2/M phase and apoptosis as illustrated by 25.4 % of the total cells accumulating in the apoptotic sub-G1 phase. The flow cytometric data clearly indicated that compound **2y** possessed the capacity of dysregulation of cell cycle progression and induction of apoptosis in HCT116 cells.

< Insert Fig. **2**>

2.4. Kinase inhibitory assays

To elucidate the molecular target of this new class of compounds, profiling of representative compounds, including **2d**, **2g** and **2y**, was carried out over a panel of eight kinases. As a result, they were identified to be Aurora A inhibitors with respective IC_{50} values of 32 nM, 46 nM, and 519 nM.

Aurora A kinase, a conserved serine/threonine kinase locates mainly to the centrosomes, is responsible for mitotic entry and exit, centrosome maturation, separation, and bipolar spindle assembly.[7] There are accumulating experimental results illustrating the intimate roles played by overexpression of Aurora A in genomic instability and tumorigenesis.[8] In contrast, inhibition of Aurora A kinase would induce G2/M tumor cell cycle delay and subsequent apoptotic cell death, which make it a viable anticancer target for solid tumors and hematological malignancies, including primary colon, breast cancers, and leukemias.[9] Until now, a variety of small-molecule inhibitors of Aurora A, as exemplified by VX-680 (MK-0457), PHA-739358, SNS-314, CYC-116, AZD1152, MLN8054 and MLN8237, have been advanced into clinical evaluation stage. Hence, the discovery of **2d**, **2g** and **2y** as potential Aurora A kinase inhibitors is meaningful and elicits our further research in this area.

As shown in Table **3**, derivatives **2d** and **2g** which only differed in a chlorine substituent on the phenyl ring displayed comparable inhibitory activities against Aurora A and were over 10-fold more effective relative to the most cytotoxic compound **2y**. The factors attributing to such incompatible results between the cytotoxicity and enzymatic assay might be multifarious, such as impaired cellular uptake, metabolism, and/or off target activities unrelated to cancer cell growth and apoptosis. Interestingly, we did found some discrepancy in cell permeability of these compounds that could to some extent explained the consequence (Table **S2**). Clearly, replacement of the hydrophilic morpholine of compound **1** by more lipophilic phenyl rings in our compounds **2d**, **2g** and **2y** abolished CHK1 inhibitory potency, which was consistent with the fact that simultaneous inhibition of CHK1 and other cell cycle associated kinases may result in counterproductive effects in the cell cycle control.[10] As expected, these compounds also demonstrated significant selectivity over other kinases namely CDK2, MEK1, GSK3β, BRAF, IKKβ, and PKC.

< Insert Table **3**>

2.5. Molecular docking study

To gain better understanding of the interactions of **2d** and **2y** with Aurora A protein, we conducted a molecular docking study utilizing C-DOCKER program within Discovery Studio 2.5. The binding modes of compounds **2d** and **2y** bound to Aurora A kinase were depicted in Fig. **3A** and Fig. **3B**, respectively. Both compounds **2d** and **2y** occupied the ATP binding site of Aurora A kinase via substantial hydrophobic contacts with a number of neighboring hydrophobic residues, and the binding was stabilized by the hydrogen bonding network with the hinge backbone Ala213 and Glu211 as expected. The C5 attachments in **2d** and **2y** with corresponding amide and urea linkages allowed the phenyl ring extending into the solvent front. Besides, an additional contact between the amide carbonyl oxygen and Arg220 was observed in **2d**. As for **2y**, the urea carbonyl oxygen located too far to generate hydrogen bond contact with the Arg220 residue as **2d** did, which suggested that the 5-amide linkage was beneficial for adopting an appropriate orientation so as to confer additional interactions with the kinase and increase binding affinity.

< Insert Fig. **3A** > < Insert Fig. **3B** >

3. Conclusions

A series of novel 3-(pyrrolopyridin-2-yl)indazoles was synthesized and evaluated for their anti-proliferative activities against five human cancer cell lines. All of them exhibited vigorous potency against HL60 cell line with IC_{50} values ranging from singe digital nanomolar to micromolar level. Besides, a majority of them displayed modest to good antiproliferative activities against the other four cell lines, including KB, SMMC-7721, HCT116, and A549. In particular, compound **2y**, as the most distinguished one (IC_{50} values of 8.3 nM and 1.3 nM against HL60 and HCT116, respectively) in this series, induced cell cycle arrest at G2/M phase and apoptosis in a cell cycle profile (FACS) analysis. To elucidate the molecular target underlying this result, in vitro biochemical assays were conducted for the representative compounds **2d**, **2g** and **2y**. Of the eight kinases being tested, good inhibitory activities were obtained against Aurora A at the nanomolar level and almost no inhibitory efficacy has been observed against seven other kinase targets. Furthermore, the binding modes of derivatives **2d** and **2y** bound to Aurora A were explored using in silico docking. These findings will facilitate the development of potent pyrrolopyridin-indazoles as a novel class of Aurora A inhibitors. And further structure optimization work such as addressing the solubility issue to improve the physical chemical properties will be reported in the near future.

4. Experimental

4.1. Chemistry

Melting points were determined with a B-540 Büchi melting-point apparatus and are uncorrected. ^{1}H NMR spectra were recorded on a 500 MHz, ^{13}C NMR were recorded on a 125 MHz spectrometer at room temperature (chemical shifts are given in ppm (δ) relative to TMS as internal standard, coupling constants (J) are in hertz (Hz), and signals are designated as follows: s, singlet; d, doublet; t, triplet; m, multiplet; br, broad singlet, etc.). Mass spectra (MS), ESI (positive) were recorded on an Esquire-LC-00075 spectrometer. Thin layer chromatography was carried out using plate silica gel F254 Merck. Reagents and solvents were purchased from common commercial suppliers and some unhydrous solvents were further purified before usage. All yields are unoptimized and generally represent the result of a single experiment.

4.1.1. General procedure for the synthesis of indazole intermediates (4a-c).

$NaNO_2$ aqueous solution (13.80 g, 0.2 mol, 32.20 mL) was added dropwise to a mixture of **3a** (21.40 g, 0.2 mol), H_2O (190 mL), and 12 N HCl aqueous solution (50 mL, 0.6 mol) at 0 ^{o}C. The mixture was stirred at 0 ^{o}C for 30 min and then was filtered. The precooled $NaBF_4$ (24.20 g, 0.22 mol) dissolved in H_2O (90 mL) was added to the filtrate and kept stirring at 0 ^{o}C for an additional 40 min. The precipitate was collected by filtration, washed with cold ethanol (50 mL×3), cold ethyl ether (50 mL×3), and concentrated in vacuo to deliver diazonium salt (19.19 g) as a yellow solid. To a solution of diazonium salt (19.19 g, 0.093 mol) in $CHCl_3$ (231 mL), KOAc (15.15 g, 0.155 mol) was added. The mixture was stirred at room temperature for 4 h. Afterwards, the reaction was quenched with water (200 mL) and extracted with CH_2Cl_2 (70 mL×3). The organic phase was washed with brine (50 mL×3), dried over anhydrous Na_2SO_4, and concentrated under reduced pressure. The obtained crude residue was purified by recrystallization to give the title compound 7.51 g.

4.1.1.1. 1*H*-Indazole (4a). Brown solid (75%), mp: 148-150 ^{o}C. ^{1}H NMR (500 MHz, DMSO-d_6) δ 13.05 (s, 1H), 8.06 (s, 1H), 7.70 (d, 1H, J = 8.0 Hz), 7.53 (d, 1H, J = 8.0 Hz), 7.34 (t, 1H, J = 7.6 Hz), 7.10 (t, 1H, J = 7.6 Hz). ESI-MS: m/z = 119 $[M+1]^+$.

4.1.1.2. 6-Chloro-1*H*-indazole (4b). Yellow solid (65%), mp: 172-174 °C (lit. 175-176 °C).

4.1.1.3. 1*H*-Indazole-6-carbonitrile (4c). Yellow solid (53%), mp: 127-129 °C. ^{1}H NMR (500 MHz, DMSO-d_6) δ 13.64 (s, 1H), 8.28 (s, 1H), 8.17 (s, 1H), 7.99 (d, 1H, J = 8.0 Hz), 7.45 (d, 1H, J = 8.0 Hz). ESI-MS: m/z = 144 $[M+1]^+$.

4.1.2. General procedure for the synthesis of 3-iodo-1*H*-indazoles (5a-c).

KOH (31.10 g, 0.555 mol) was added in portions at 0 °C to a solution of **4a** (15.80 g, 0.134 mol) and I_2 (85.40 g, 0.336 mol) in DMF (263.40 mL). The mixture was stirred for 4 h at room temperature, quenched with saturated $Na_2S_2O_3$ solution (50 mL), diluted with H_2O (150 mL), and extracted with EtOAc (70 mL×3). The organic phase was washed with brine (50 mL×3), dried over anhydrous Na_2SO_4, and concentrated under reduced pressure. The obtained residue was purified by silica gel column chromatography (petroleum ether/ethyl acetate = 15:1, v/v) to give an orange solid (16.78 g).

4.1.2.1. 3-Iodo-1*H*-indazole (5a). Orange solid (52%), mp: 142-143 °C. ^{1}H NMR (500 MHz, DMSO-d_6) δ 13.50 (s, 1H), 7.55 (d, 1H, J = 8.4 Hz), 7.43 (d, 1H, J = 8.4 Hz), 7.43 (t, 1H, J = 7.2 Hz), 7.20 (t, 1H, J = 7.2 Hz). ESI-MS: m/z = 245 $[M+1]^+$.

4.1.2.2. 6-Chloro-3-iodo-1*H*-indazole (5b). Orange solid (51%), mp: 162-165 °C. ^{1}H NMR (500 MHz, DMSO-d_6) δ 13.39 (s, 1H), 7.70 (s, 1H), 7.56 (d, 1H, J = 8.5 Hz), 7.45 (d, 1H, J = 8.5 Hz). ESI-MS: m/z = 279 $[M+1]^+$.

4.1.2.3. 3-Iodo-1*H*-indazole-6-carbonitrile (5c). Yellow solid (47%), mp: 259 °C (dec). ^{1}H NMR (500 MHz, DMSO-d_6) δ 14.06 (s, 1H), 8.20 (s, 1H), 7.62 (d, 1H, J = 8.5 Hz), 7.49 (d, 1H, J = 8.5 Hz). ESI-MS: m/z = 270 $[M+1]^+$.

4.1.3. General procedure for the synthesis of 3-(tributylstannyl)-1*H*-indazoles (6a-c).

Bromoethane (9 mL, 121 mmol) was added slowly to a solution of magnesium (2.70 g, 112.5 mmol) and I_2 (catalytic amount) in dry ethyl ether (114 mL) at 0 °C under N_2 atmosphere. Until the magnesium being completely consumed, 3-iodo-indazole (7.59 g, 31.1 mmol) dissolved in THF (190 mL) was added dropwise to the solution. The mixture was stirred at 0 °C for 30 min. Then a solution of tributylstannanylium chloride (41.80 g, 128 mmol) in THF (10 mL) was added dropwise. The mixture was stirred at 0 °C for an additional 40 min, quenched with saturated NH_4Cl solution, diluted with H_2O (70 mL), and extracted with EtOAc (30 mL×3). The organic phase was washed with brine (20 mL×3), dried over anhydrous Na_2SO_4, and concentrated under reduced pressure. The obtained mixture was purified by silica gel column chromatography (petroleum ether/ethyl acetate = 10:1, v/v) to give the title compound as a yellow liquid (7.73 g).

4.1.3.1. 3-(Tributylstannyl)-1*H*-indazole (6a). Yellow oil (61%). ^{1}H NMR (500 MHz, DMSO-d_6) δ 11.05 (s, 1H), 7.76 (d, 1H, J = 8.4 Hz), 7.55 (d, 1H, J = 8.4 Hz), 7.37 (t, 1H, J = 7.6 Hz), 7.15 (t, 1H, J = 7.6 Hz), 1.56 (m, 6H), 1.33 (m, 6H), 1.27 (t, 6H, J = 8.8 Hz), 0.90 (t, 9H, J = 7.2 Hz). ESI-MS: m/z = 409 $[M+1]^+$.

4.1.3.2. 6-Chloro-3-(tributylstannyl)-1*H*-indazole (6b). Yellow oil (53%). ^{1}H NMR (500 MHz, DMSO-d_6) δ 13.39 (s, 1H), 7.62 (d, 2H, J = 8.5 Hz), 7.04 (d, 1H, J = 8.5 Hz), 1.48 (m, 6H), 1.25 (q, 6H,

J = 7.5 Hz), 1.12 (m, 6H), 0.79 (t, 9H, *J* = 7.5 Hz). ESI-MS: m/z = 443 $[M+1]^+$.

4.1.3.3. 3-(Tributylstannyl)-1*H*-indazole-6-carbonitrile (6c). Yellow oil (45%). ^{1}H NMR (500 MHz, DMSO-d_6) δ 13.39 (s, 1H), 8.12 (d, 2H, *J* = 8.5 Hz), 7.64 (d, 1H, *J* = 8.5 Hz), 1.58 (m, 6H), 1.35 (q, 6H, *J* = 7.5 Hz), 1.22 (m, 6H), 0.79 (t, 9H, *J* = 7.5 Hz). ESI-MS: m/z = 434 $[M+1]^+$.

4.1.4. General procedure for the synthesis of Boc-protected indazoles (7a-c).

$(Boc)_2O$ (4.91 g, 22.50 mmol) was added to a solution of **6a** (7.73 g, 18.90 mmol) and DMAP (46.30 mg, 0.38 mmol) in THF (88.80 mL). The mixture was stirred for 30 min at room temperature, concentrated under reduced pressure and subjected to silica gel column chromatography (petroleum ether/ethyl acetate = 25:1, v/v) to yield a yellow liquid (6.48 g).

4.1.4.1. Tert-butyl 3-(tributylstannyl)-1*H*-indazole-1-carboxylate (7a). Yellow oil (68%). ^{1}H NMR (500 MHz, $CDCl_3$) δ 8.05 (d, 1H, *J* = 8.0 Hz), 7.71 (d, 1H, *J* = 8.0 Hz), 7.52 (t, 1H, *J* = 7.5 Hz), 7.31 (t, 1H, *J* = 7.5 Hz), 1.63 (s, 9H), 1.55 (m, 6H), 1.26 (q, 6H, *J* = 7.5 Hz), 1.19 (t, 6H, *J* = 7.5 Hz), 0.81 (t, 9H, *J* = 7.5 Hz). ESI-MS: m/z = 509 $[M+1]^+$.

4.1.4.2. Tert-butyl 6-chloro-3-(tributylstannyl)-1*H*-indazole-1-carboxylate (7b). Yellow oil (63%). ^{1}H NMR (500 MHz, $CDCl_3$) δ 8.15 (s, 1H), 7.55 (d, 1H, *J* = 9.0 Hz), 7.24 (d, 1H, *J* = 9.0 Hz), 1.72 (s, 9H), 1.57 (m, 6H), 1.32 (q, 6H, *J* = 7.0 Hz), 1.24 (t, 6H, *J* = 8.0 Hz), 0.87 (t, 9H, *J* = 7.0 Hz). ESI-MS: m/z = 543 $[M+1]^+$.

4.1.4.3. Tert-butyl 6-cyano-3-(tributylstannyl)-1*H*-indazole-1-carboxylate (7c). Yellow oil (58%). ^{1}H NMR (500 MHz, $CDCl_3$) δ 8.65 (s, 1H), 8.15 (d, 1H, *J* = 9.0 Hz), 7.34 (d, 1H, *J* = 9.0 Hz), 1.72 (s, 9H), 1.67 (m, 6H), 1.42 (q, 6H, *J* = 7.0 Hz), 1.34 (t, 6H, *J* = 8.0 Hz), 0.87 (t, 9H, *J* = 7.0 Hz). ESI-MS: m/z = 534 $[M+1]^+$.

4.1.5. Synthesis of indazole 6-methyl-5-nitropyridin-2-amine (9).

The 6-methylpyridin-2-amine (20 g, 185mmol) was dissolved in 98% H_2SO_4 (91 mL). A mixture of fuming HNO_3 (9 mL) and 98% H_2SO_4 (9 mL) was added dropwise to the vigorously stirring solution over 30 min at -6 ^{o}C. The mixture was stirred for 2 h at 0 ^{o}C and slowly warmed to 10 ^{o}C over 1 h and kept stirring for an additional hour. Afterwards, the solution was warmed to 20 °C over 1 h and stirred for 2 h. The reaction mixture was poured onto ice and basified with ammonium hydroxide (pH ~ 9). The precipitated solid was collected by filtration and purified by steam distillation to afford compound **9** (9.99 g). Yellow solid (36%), mp: 189-191 ^{o}C. ^{1}H NMR (500 MHz, DMSO-d_6) δ 7.77 (d, 1H, *J* = 9.2 Hz), 6.09 (d, 1H, *J* = 9.2 Hz), 6.11 (s, 2H), 2.36 (s, 3H). ESI-MS: m/z = 154 $[M+1]^+$.

4.1.6. Synthesis of tert-butyl (6-methyl-5-nitropyridin-2-yl) carbamate (10).

$(Boc)_2O$ (16.94 g, 77.62 mmol) was added to a solution of **9** (9.99 g, 65.2 mmol) and DMAP (160.2 mg, 1.31 mmol) in THF (306 mL). After stirring at room temperature for 30 min, THF was removed under reduced pressure. The obtained crude product was purified by chromatography (petroleum ether/ethyl acetate = 25:1, v/v) to afford compound **10** (14.3 g). White solid (87%), mp: 127-129 ^{o}C. ^{1}H NMR (500 MHz, DMSO-d_6) δ 10.52 (s, 1H), 8.41 (d, 1H, *J* = 8.8 Hz), 7.84 (d, 1H, *J* = 8.8 Hz), 2.67 (s, 3H), 1.46 (s, 9H). ESI-MS: m/z = 254 $[M+1]^+$.

4.1.7. Synthesis of tert-butyl methyl (6-methyl-5-nitropyridin-2-yl) carbamate (11).

NaH (3.11 g, 130 mmol) was added in portions to a solution of **10** (14.3 g, 56.50 mmol) in dry DMF (172 mL) at -5 °C. After stirring for 40 min, iodomethane (4.17 mL, 66.98 mmol) was added dropwise over 30 min and stirred for 1 h at room temperature. H_2O (200 mL) was added and the resulting solution was extracted with ethyl acetate (70 mL×3), washed with brine (50 mL×3), dried over anhydrous Na_2SO_4, and concentrated under reduced pressure. The obtained residue was purified by chromatography (petroleum ether/ethyl acetate = 25:1, v/v) to afford **11** (9.52 g). Yellow solid (58%), mp: 141-143 °C. ^{1}H NMR (500 MHz, DMSO-d_6) δ 8.39 (d, 1H, J = 9.2 Hz), 7.84 (d, 1H, J = 9.2 Hz), 3.39 (s, 3H), 2.73 (s, 3H), 1.50 (s, 9H). ESI-MS: m/z = 268 $[M+1]^+$.

4.1.8. Synthesis of tert-butyl methyl (1*H*-pyrrolo[3,2-b]pyridin-5-yl) carbamate (12).

DMFDMA (20.38 g, 171 mmol) was added to a solution of **11** (21.85 g, 81.80 mmol) in DMF (278 mL) and stirred at 95 °C for 5 h. Then the solvent was removed under reduced pressure. The obtained crude product was subjected to chromatography (petroleum ether/ethyl acetate = 10:1, v/v). The obtained intermediate was dissolved in MeOH (450 mL) and was added 10% Pd/C (0.29 g). The mixture was stirred at room temperature overnight under H_2 atmosphere. After filtration through Celite® and concentration under vacuo, the obtained crude product was recrystallized from EtOH to give **12** (13.91 g). White solid (69%), mp: 157-159 °C. ^{1}H NMR (500 MHz, DMSO-d_6) δ 11.30 (s, 1H), 7.73 (d, 1H, J = 8.8 Hz), 7.60 (d, 1H, J = 3.2 Hz), 7.17 (d, 1H, J = 8.8 Hz), 6.45 (d, 1H, J = 3.2 Hz), 3.27 (s, 3H), 1.42 (s, 9H). ESI-MS: m/z = 248 $[M+1]^+$.

4.1.9. Synthesis of tert-butyl 5-((tert-butoxycarbonyl)(methyl)amino)-1*H*-pyrrolo[3,2-b]-pyridine-1-carboxylate (13).

$(Boc)_2O$ (14.6 g, 66.90 mmol) was added to a solution of **12** (13.91 g, 56.2 mmol) and DMAP (138.0 mg, 1.13 mmol) in THF (264 mL). After stirring at room temperature for 30 min, THF was removed under reduced pressure. The obtained crude product was purified by chromatography (petroleum ether/ethyl acetate = 20:1, v/v) to afford compound **13** (14.3 g). White solid (77%), mp: 157-159 °C. ^{1}H NMR (500 MHz, $CDCl_3$) δ 8.26 (d, J = 8.8 Hz, 1H), 7.77 (d, J = 3.6 Hz, 1H), 7.44 (d, 1H, J = 8.8 Hz), 6.67 (d, 1H, J = 3.6 Hz), 3.41 (s, 3H), 1.65 (s, 9H), 1.48 (s, 9H). ESI-MS: m/z = 348 $[M+1]^+$.

4.1.10. Synthesis of tert-butyl 5-((tert-butoxycarbonyl)(methyl)amino)-2-iodo-1*H*-pyrrolo-[3,2-b]pyridine-1-carboxylate (14).

N-butyllithium (2.5 mol/L, 9.2 mL) was added dropwise to a solution of **13** (6.6 g, 19.0 mmol) in dry THF (60 mL) at -78 °C over 30 min under N_2 atmosphere. The mixture was allowed to warm to -60 °C and stirred for 1 h. Then a solution of I_2 (5.3 g) dissolved in dry THF (40 mL) was slowly added at -72 °C. The reaction was stirred at -72 °C for 2 h and stirred at room temperature for 1 h, quenched with saturated $Na_2S_2O_3$ (50 mL), diluted with H_2O (100 mL), extracted with ethyl acetate (50 mL×3), and washed with brine (30 mL×3). The solvent was dried over anhydrous Na_2SO_4, and concentrated under reduced pressure. The obtained residue was purified by chromatography (petroleum ether/acetone = 15:1, v/v) to afford **14** (5.42 g). Yellow oil (61%). ^{1}H NMR (500 MHz, DMSO-d_6) δ 8.19 (d, 1H, J = 8.8 Hz), 7.42 (d, 1H, J = 8.8 Hz), 6.35 (s, 1H), 3.28 (s, 3H), 1.66 (s, 9H), 1.43 (s, 9H). ESI-MS: m/z = 474 $[M+1]^+$.

4.1.11. General procedure for the synthesis of 15a-c.

Compound **7a** (3.14 g, 6.18 mmol) in toluene (10 mL) was added dropwise to a mixture of **14** (2.75 g, 5.81 mmol), $Pd(PPh_3)_4$ (0.67 g, 0.581 mmol), CuI (0.15 g, 0.79 mmol) in toluene (110 mL) under N_2 atmosphere and stirred at 95 °C for 24 h. The reaction mixture was cooled to room temperature and filtered. The filtrate was concentrated under reduced pressure and followed by purification through chromatography (petroleum ether/acetone = 15:1, v/v) to afford **15a** (3.35 g).

4.1.11.1. Tert-butyl 3-(1-(tert-butoxycarbonyl)-5-((tert-butoxycarbonyl)(methyl)amino)-1*H*-pyrrolo[3,2-b]pyridin-2-yl)-1*H*-indazole-1-carboxylate (15a). Yellow oil (63%). ^{1}H NMR (500 MHz, DMSO-d_6) δ 8.42 (d, 1H, J = 7.2 Hz), 8.18 (d, 1H, J = 6.4 Hz), 7.78 (d, 1H, J = 6.4 Hz), 7.67 (t, 1H, J = 6.4 Hz), 7.64 (d, 1H, J = 7.2 Hz), 7.43 (t, 1H, J = 6.4 Hz), 7.20 (s, 1H), 3.35 (s, 3H), 1.66 (s, 9H), 1.47 (s, 9H), 1.14 (s, 9H). ESI-MS: m/z = 564 $[M+1]^+$.

4.1.11.2. Tert-butyl 3-(1-(tert-butoxycarbonyl)-5-((tert-butoxycarbonyl)(methyl)amino)-1*H*-pyrrolo[3,2-b]pyridin-2-yl)-6-chloro-1*H*-indazole-1-carboxylate (15b). Yellow oil (56%). ^{1}H NMR (500 MHz, DMSO-d_6) δ 8.44 (d, 1H, J = 9.5 Hz), 8.29 (s, 1H), 7.59 (d, 1H, J = 9.5 Hz), 7.54 (d, 1H, J = 8.5 Hz), 7.32 (d, 1H, J = 8.5 Hz), 7.04 (s, 1H), 3.46 (s, 3H), 1.73 (s, 9H), 1.52 (s, 9H), 1.24 (s, 9H). ESI-MS: m/z = 598 $[M+1]^+$.

4.1.11.3. Tert-butyl 3-(1-(tert-butoxycarbonyl)-5-((tert-butoxycarbonyl)(methyl)amino)-1*H*-pyrrolo[3,2-b]pyridin-2-yl)-6-cyano-1*H*-indazole-1-carboxylate (15c). Yellow oil (35%). ^{1}H NMR (500 MHz, DMSO-d_6) δ 8.43 (d, 1H, J = 9.0 Hz), 8.32 (s, 1H), 7.94 (d, 1H, 8.5 Hz), 7.62 (d, 1H, J = 9.0 Hz), 7.55 (d, 1H, J = 8.5 Hz), 7.10 (s, 1H), 3.38 (s, 3H), 1.71 (s, 9H), 1.51 (s, 9H), 1.17 (s, 9H). ESI-MS: m/z = 589 $[M+1]^+$.

4.1.12. General procedure for the synthesis of 16a-c.

12 N HCl aqueous solution (37 mL) was added dropwise to a solution of **15a** (1.55 g, 2.75 mmol) in EtOH (37 mL). The mixture was stirred at room temperature for 5 h. Then 10% NaOH aqueous solution was added to the solution to basify the mixture to neutral. The mixture was extracted with ethyl acetate (50 mL×3), washed with brine (30 mL×3), dried over anhydrous Na_2SO_4, and concentrated under reduced pressure. The obtained residue was purified by chromatography (petroleum ether/ethanol = 3:1, v/v) to afford **16a** (0.3 g).

4.1.12.1. 2-(1*H*-Indazol-3-yl)-*N*-methyl-1*H*-pyrrolo[3,2-b]pyridin-5-amine (16a).
White solid (42%), mp: 244-246 °C. ^{1}H NMR (500 MHz, DMSO-d_6) δ 13.27 (s, 1H), 11.25 (s, 1H), 8.18 (d, 1H, J = 8.4 Hz), 7.59 (d, 1H, J = 8.0 Hz), 7.46 (d, 1H, J = 8.0 Hz), 7.42 (t, 1H, J = 7.2 Hz), 7.23 (t, 1H, J = 7.2 Hz), 6.92 (s, 1H), 6.35 (d, 1H, J = 8.4 Hz), 6.04 (q, 1H, 4.8 Hz), 2.81 (d, 3H, J = 4.8 Hz). ESI-MS: m/z = 264 $[M+1]^+$.

4.1.12.2. 2-(6-Chloro-1*H*-indazol-3-yl)-*N*-methyl-1*H*-pyrrolo[3,2-b]pyridin-5-amine (16b). Yellow solid (39%), mp: 250 °C (dec). ^{1}H NMR (500 MHz, DMSO-d_6) δ 13.37 (s, 1H), 11.26 (s, 1H), 8.19 (d, 1H, J = 8.5 Hz), 7.65 (s, 1H), 7.44 (d, 1H, J = 9.0 Hz), 7.20 (d, 1H, J = 9.0 Hz), 6.93 (s, 1H), 6.34 (d, 1H, J = 8.5 Hz), 6.02 (q, 1H, J = 4.5 Hz), 2.81 (d, 3H, J = 4.5 Hz). ESI-MS: m/z = 298 $[M+1]^+$.

4.1.12.3. 3-(5-(Methylamino)-1*H*-pyrrolo[3,2-b]pyridin-2-yl)-1*H*-indazole-6-carbonitrile

(16c). Yellow solid (43%), mp: 250 °C (dec). ^{1}H NMR (500 MHz, DMSO-d_6) δ 13.45 (s, 1H), 11.40 (s, 1H), 8.41 (d, 1H, J = 8.0 Hz), 8.26 (s, 1H), 7.53 (d, 1H, J = 9.0 Hz), 7.49 (d, 1H, J = 9.0 Hz), 7.01 (s, 1H), 6.39 (d, 1H, J = 8.5 Hz), 6.10 (q, 1H, J = 5.0 Hz), 2.85 (d, 3H, J = 5.0 Hz). ESI-MS: m/z = 289 $[M+1]^+$.

4.1.13. General procedure for the synthesis of 2a-x.

A mixture of **16a** (26.30 mg, 0.10 mmol), acetyl chloride (7.80 mg, 0.10 mmol), and pyridine (2.0 mL) was stirred at 60 °C and monitored by TLC. Pyridine was removed under reduced pressure. Then the mixture was basified by 1 N NaOH aqueous solution (pH ~ 9), extracted with CH_2Cl_2 (20 mL×3), washed with brine (5 mL×3), dried over anhydrous Na_2SO_4, and concentrated under reduced pressure. The obtained residue was purified by chromatography (petroleum ether/ethanol = 8:1, v/v) to afford **2a** (0.3 g).

4.1.13.1. *N*-(2-(1*H*-Indazol-3-yl)-1*H*-pyrrolo[3,2-b]pyridin-5-yl)-*N*-methylacetamide (2a). Yellow solid (43%), mp: 275 °C (dec). ^{1}H NMR (500 MHz, DMSO-d_6) δ 13.66 (s, 1H), 12.02 (s, 1H), 8.23 (d, 1H, J = 8.4 Hz), 7.84 (d, 1H, J = 8.4 Hz), 7.63 (d, 1H, J = 8.4 Hz), 7.44 (t, 1H, J = 7.2 Hz), 7.26 (t, 1H, J = 7.2 Hz), 7.24 (s, 1H), 7.13 (d, 1H, J = 8.0 Hz), 3.25 (s, 3H), 1.89 (s, 3H). ESI-MS: m/z = 306 $[M+1]^+$.

4.1.13.2. *N*-(2-(1*H*-Indazol-3-yl)-1*H*-pyrrolo[3,2-b]pyridin-5-yl)-*N*-methylpropionamide (2b). Yellow solid (51%), mp: 219-221 °C. ^{1}H NMR (500 MHz, DMSO-d_6) δ 13.55 (s, 1H), 12.02 (s, 1H), 8.27 (d, 1H, J = 8.0 Hz), 7.89 (d, 1H, J = 8.5 Hz), 7.67 (d, 1H, J = 8.5 Hz), 7.49 (t, 1H, J = 7.5 Hz), 7.31 (t, 1H, J = 8.0 Hz), 7.29 (s, 1H), 7.16 (d, 1H, J = 8.0 Hz), 3.83 (s, 3H), 2.19 (q, 2H, J = 7.5 Hz), 0.98 (t, 3H, J = 7.5 Hz). ESI-MS: m/z = 320 $[M+1]^+$.

4.1.13.3. *N*-(2-(1*H*-Indazol-3-yl)-1*H*-pyrrolo[3,2-b]pyridin-5-yl)-*N*-methylpivalamide (2c). Yellow solid (77%), mp: 260 °C (dec). ^{1}H NMR (500 MHz, DMSO-d_6) δ 13.67 (s, 1H), 12.03 (s, 1H), 8.23 (d, 1H, J = 8.4 Hz), 7.84 (d, 1H, J = 8.0 Hz), 7.63 (d, 1H, J = 8.4 Hz), 7.44 (t, 1H, J = 7.6 Hz), 7.25 (t, 1H, J = 7.6 Hz), 7.23 (s, 1H), 7.11 (d, 1H, J = 8.0 Hz), 3.16 (s, 3H), 0.96 (s, 9H). ESI-MS: m/z = 348 $[M+1]^+$.

4.1.13.4. *N*-(2-(1*H*-Indazol-3-yl)-1*H*-pyrrolo[3,2-b]pyridin-5-yl)-4-chloro-*N*-methylbenzamide (2d). White solid (67%), mp: 178-180 °C. ^{1}H NMR (500 MHz, DMSO-d_6) δ 13.51 (s, 1H), 11.90 (s, 1H), 8.22 (d, 1H, J = 8.0 Hz), 7.62 (d, 1H, J = 8.4 Hz), 7.57 (d, 1H, J = 8.8 Hz), 7.44 (t, 1H, J = 7.2 Hz), 7.23 (m, 4H), 7.17 (m, 3H), 6.75 (d, 1H, J = 8.4 Hz), 3.48 (s, 3H). ESI-MS: m/z = 368 $[M+1]^+$.

4.1.13.5. *N*-(2-(1*H*-Indazol-3-yl)-1*H*-pyrrolo[3,2-b]pyridin-5-yl)-*N*-methyl-3-phenylpropanamide (2e). Yellow solid (49%), mp: 86-88 °C. ^{1}H NMR (500 MHz, DMSO-d_6) δ 11.98 (br, 1H), 11.52 (s, 1H), 8.22 (d, 1H, J = 6.5 Hz), 7.82 (d, 1H, J = 8.5 Hz), 7.63 (d, 1H, J = 8.5 Hz), 7.43 (t, 1H, J = 7.5 Hz), 7.25 (t, 1H, J = 7.5 Hz), 7.22 (s, 1H), 7.16 (m, 2H), 7.03 (m, 4H), 3.25 (s, 3H), 2.79 (t, 2H, J = 8.0 Hz), 2.40 (t, 2H, J = 8.0 Hz). ESI-MS: m/z = 396 $[M+1]^+$.

4.1.13.6. *N*-(2-(1*H*-Indazol-3-yl)-1*H*-pyrrolo[3,2-b]pyridin-5-yl)-4-fluoro-*N*-methylbenzamide (2f). Yellow solid (19%), mp: 162-164 °C. ^{1}H NMR (500 MHz, DMSO-d_6) δ 10.45 (br, 1H), 9.27 (s, 1H), 8.16 (d, 1H, J = 8.0 Hz), 7.60 (d, 1H, J = 8.5 Hz), 7.53 (t, 1H, J = 8.5 Hz), 7.51 (d, 1H, J = 8.5 Hz),

7.42 (t, 2H, *J* = 5.5 Hz), 7.39 (t, 1H, *J* = 7.5 Hz), 7.43 (s, 1H), 6.86 (t, 2H, *J* = 8.5 Hz), 6.65 (d, 1H, *J* = 8.0 Hz), 3.71 (s, 3H). ESI-MS: m/z = 386 $[M+1]^+$.

4.1.13.7. *N*-(2-(1*H*-Indazol-3-yl)-1*H*-pyrrolo[3,2-b]pyridin-5-yl)-4-chloro-*N*-methylbenzamide (2g). White solid (27%), mp: 260-262 °C. ^{1}H NMR (500 MHz, DMSO-d_6) δ 13.60 (s, 1H), 11.94 (s, 1H), 8.22 (d, 1H, *J* = 7.6 Hz), 7.62 (dd, 2H, *J* = 2.8 Hz, 8.0 Hz), 7.43 (t, 1H, *J* = 7.2 Hz), 7.25 (m, 5H), 7.19 (s, 1H), 6.79 (d, 1H, *J* = 8.4 Hz), 3.47 (s, 3H); ^{13}C NMR (125 MHz, DMSO-d_6) δ 168.57, 150.11, 145.39, 141.35, 136.62, 135.97, 135.51, 134.19, 130.00, 127.89, 127.65, 126.59, 121.51, 120.56, 120.02, 115.21, 110.69, 99.66, 36.39. ESI-MS: m/z = 402 $[M+1]^+$.

4.1.13.8. *N*-(2-(1*H*-Indazol-3-yl)-1*H*-pyrrolo[3,2-b]pyridin-5-yl)-4-bromo-*N*-methylbenzamide (2h). Yellow solid (38%), mp: 272 °C (dec). ^{1}H NMR (500 MHz, DMSO-d_6) δ 13.61 (s, 1H), 11.94 (s, 1H), 8.22 (d, 1H, *J* = 8.0 Hz), 7.63 (d, 2H, *J* = 8.5 Hz), 7.46 (t, 1H, *J* = 7.0 Hz), 7.41 (dd, 2H, *J* = 1.5 Hz, 6.5 Hz), 7.26 (t, 1H, *J* = 7.0 Hz), 7.21 (dd, 2H, *J* = 2.0 Hz, *J* = 7.0 Hz), 7.19 (s, 1H), 6.80 (d, 1H, *J* = 10.5 Hz), 3.47 (s, 1H). ESI-MS: m/z = 446 $[M+1]^+$.

4.1.13.9. *N*-(2-(1*H*-Indazol-3-yl)-1*H*-pyrrolo[3,2-b]pyridin-5-yl)-4-methoxy-*N*-methylbenzamide (2i). Yellow solid (44%), mp: 265 °C (dec). ^{1}H NMR (500 MHz, DMSO-d_6) δ 13.60 (s, 1H), 11.92 (s, 1H), 8.22 (d, 1H, *J* = 8.4 Hz), 7.63 (d, 1H, *J* = 8.4 Hz), 7.60 (d, 1H, *J* = 8.8 Hz), 7.43 (t, 1H, *J* = 7.2 Hz), 7.25 (t, 1H, *J* = 7.2 Hz), 7.24 (s, 1H), 7.21 (d, 2H, *J* = 2.8 Hz), 6.71 (m, 3H), 3.66 (s, 3H), 3.45 (s, 3H). ESI-MS: m/z = 398 $[M+1]^+$.

4.1.13.10. *N*-(2-(1*H*-Indazol-3-yl)-1*H*-pyrrolo[3,2-b]pyridin-5-yl)-3-methoxy-*N*-methylbenzamide (2j). Yellow solid (45%), mp: 152-154 °C. ^{1}H NMR (500 MHz, DMSO-d_6) δ 13.57 (s, 1H), 11.90 (s, 1H), 7.23 (d, 1H, *J* = 8.0 Hz), 7.63 (d, 1H, *J* = 8.5 Hz), 7.60 (d, 1H, *J* = 8.5 Hz), 7.45 (t, 1H, *J* = 7.5 Hz), 7.26 (t, 1H, *J* = 7.5 Hz), 7.21 (s, 1H), 7.09 (t, 1H, *J* = 8.0 Hz), 6.85 (t, 1H, *J* = 2.0 Hz), 6.81 (m, 2H), 6.79 (d, 1H, *J* = 8.5 Hz), 3.58 (s, 3H), 3.47 (s, 3H). ESI-MS: m/z = 398 $[M+1]^+$.

4.1.13.11. *N*-(2-(1*H*-Indazol-3-yl)-1*H*-pyrrolo[3,2-b]pyridin-5-yl)-*N*-methyl-4-nitrobenzamide (2k). Yellow solid (26%), mp: 231 °C (dec). ^{1}H NMR (500 MHz, DMSO-d_6) δ 13.59 (s, 1H), 11.94 (s, 1H), 8.20 (d, 1H, *J* = 8.5 Hz), 8.05 (d, 1H, *J* = 8.5 Hz), 7.63 (t, 2H, *J* = 8.0 Hz), 7.52 (d, 2H, *J* = 9.0 Hz), 7.44 (t, 1H, *J* = 7.0 Hz), 7.16 (m, 3H), 6.91 (d, 1H, *J* = 8.0 Hz), 3.51 (s, 3H). ESI-MS: m/z = 413 $[M+1]^+$.

4.1.13.12. *N*-(2-(1*H*-Indazol-3-yl)-1*H*-pyrrolo[3,2-b]pyridin-5-yl)-*N*-methylfuran-2-carboxamide (2l). Yellow solid (45%), mp: 110-112 °C. ^{1}H NMR (500 MHz, DMSO-d_6) δ 13.59 (s, 1H), 12.00 (s, 1H), 8.22 (d, 1H, *J* = 8.0 Hz), 7.79 (d, 1H, *J* = 8.5 Hz), 7.63 (d, 1H, *J* = 8.5 Hz), 7.57 (d, 1H, *J* = 1.0 Hz), 7.44 (t, 1H, *J* = 7.5 Hz), 7.25 (t, 1H, *J* = 7.5 Hz), 7.23 (s, 1H), 7.00 (d, 1H, *J* = 8.0 Hz), 6.33 (dd, 1H, *J* =1.5 Hz, 3.5 Hz), 6.01 (d, 1H, *J* = 3.5 Hz), 3.39 (s, 3H). ESI-MS: m/z = 358 $[M+1]^+$.

4.1.13.13. *N*-(2-(6-Chloro-1*H*-indazol-3-yl)-1*H*-pyrrolo[3,2-b]pyridin-5-yl)-*N*-methylbenzamide (2m). Yellow solid (27%), mp: 275 °C (dec). ^{1}H NMR (500 MHz, DMSO-d_6) δ 13.91 (s, 1H), 12.01 (s, 1H), 7.99 (d, 1H, *J* = 8.5 Hz), 7.81 (s, 1H), 7.53 (s, 1H), 7.42 (d, 1H, *J* = 8.5 Hz), 7.29 (dd, 2H, *J* = 1.5 Hz, 9.0 Hz), 7.22 (d, 2H, *J* = 7.5 Hz), 7.14 (t, 2H, *J* = 8.0 Hz), 6.64 (d, 1H, *J* = 8.5 Hz), 3.67 (s, 3H).

ESI-MS: m/z = 402 $[M+1]^+$.

4.1.13.14. *N*-(2-(6-Cyano-1*H*-indazol-3-yl)-1*H*-pyrrolo[3,2-b]pyridin-5-yl)-*N*-methylbenzamide (2n). Yellow solid (19%), mp: 250 °C (dec). ^{1}H NMR (500 MHz, DMSO-d_6) δ 14.11 (s, 1H), 12.04 (s, 1H), 8.49 (d, 1H, J = 8.5 Hz), 8.31 (s, 1H), 7.61 (td, 2H, J = 9.0 Hz, 1.0 Hz), 7.28 (m, 4H), 7.22 (m, 2H), 6.63 (d, 1H, J = 8.0 Hz), 3.51 (s, 3H). ESI-MS: m/z = 393 $[M+1]^+$.

4.1.13.15. *N*-(2-(1*H*-Indazol-3-yl)-1*H*-pyrrolo[3,2-b]pyridin-5-yl)-*N*-methylbenzenesulfonamide (2o). Yellow solid (40%), mp: 78-80 °C. ^{1}H NMR (500 MHz, DMSO-d_6) δ 13.46 (s, 1H), 11.93 (s, 1H), 8.18 (d, 1H, J = 8.4 Hz), 7.79 (d, 1H, J = 8.4 Hz), 7.61 (m, 1H), 7.58 (d, 1H, J = 8.4 Hz), 7.49 (m, 4H), 7.39 (t, 1H, J = 8.0 Hz), 7.29 (d, 1H, J = 8.8 Hz), 7.19 (t, 1H, J = 8.0 Hz), 7.13 (d, 1H, J = 1.6 Hz), 3.20 (s, 3H). ESI-MS: m/z = 404 $[M+1]^+$.

4.1.13.16. *N*-(2-(1*H*-Indazol-3-yl)-1*H*-pyrrolo[3,2-b]pyridin-5-yl)-*N*-4-dimethylbenzenesulfonamide (2p). Yellow solid (25%), mp: 91-93 °C. ^{1}H NMR (500 MHz, DMSO-d_6) δ 13.39 (s, 1H), 11.88 (s, 1H), 8.17 (d, 1H, J = 8.0 Hz), 7.78 (d, 1H, J = 8.4 Hz), 7.58 (d, 1H, J = 8.4 Hz), 7.39 (m, 3H), 7.29 (d, 3H, J = 8.0 Hz), 7.19 (t, 1H, J = 7.6 Hz), 7.14 (d, 1H, J = 0.8 Hz), 3.18 (s, 3H), 2.76 (s, 3H). ESI-MS: m/z = 418 $[M+1]^+$.

4.1.13.17. *N*-(2-(1*H*-Indazol-3-yl)-1*H*-pyrrolo[3,2-b]pyridin-5-yl)-4-chloro-*N*-methylbenzenesulfonamide (2q). Yellow solid (40%), mp: 90-92 °C. ^{1}H NMR (500 MHz, DMSO-d_6) δ 13.50 (s, 1H), 11.98 (s, 1H), 8.22 (d, 1H, J = 8.4 Hz), 7.83 (d, 1H, J = 8.8 Hz), 7.61 (m, 3H), 7.58 (s, 1H), 7.56 (d, 1H, J = 8.4 Hz), 7.43 (t, 1H, J = 8.0 Hz), 7.29 (d, 1H, J = 8.8 Hz), 7.23 (t, 1H, J = 8.0 Hz), 7.18 (d, 1H, J = 1.2 Hz), 3.23 (s, 3H). ESI-MS: m/z = 438 $[M+1]^+$.

4.1.13.18. *N*-(2-(1*H*-Indazol-3-yl)-1*H*-pyrrolo[3,2-b]pyridin-5-yl)-4-bromo-*N*-methylbenzenesulfonamide (2r). Yellow solid (42%), mp: 80-82 °C. ^{1}H NMR (500 MHz, DMSO-d_6) δ 13.58 (s, 1H), 12.03 (s, 1H), 8.22 (d, 1H, J = 8.0 Hz), 7.84 (d, 1H, J = 8.8 Hz), 7.76 (d, 2H, J = 8.8 Hz), 7.62 (d, 1H, J = 8.4 Hz), 7.48 (d, 2H, J = 8.8 Hz), 7.43 (t, 1H, J = 8.0 Hz), 7.28 (d, 1H, J = 8.4 Hz), 7.23 (t, 1H, J = 8.0 Hz), 7.19 (s, 1H), 3.24 (s, 3H). ESI-MS: m/z = 482 $[M+1]^+$.

4.1.13.19. *N*-(2-(1*H*-Indazol-3-yl)-1*H*-pyrrolo[3,2-b]pyridin-5-yl)-4-methoxy-*N*-methylbenzenesulfonamide (2s). Yellow solid (43%), mp: 125-127 °C. ^{1}H NMR (500 MHz, DMSO-d_6) δ 13.49 (s, 1H), 11.94 (s, 1H), 8.21 (d, 1H, J = 8.8 Hz), 7.81 (d, 1H, J = 8.0 Hz), 7.61 (d, 2H, J = 8.4 Hz), 7.46 (d, 2H, J = 8.4 Hz), 7.42 (t, 1H, J = 8.0 Hz), 7.32 (d, 1H, J = 8.4 Hz), 7.22 (t, 1H, J = 8.0 Hz), 7.17 (d, 1H, J = 1.2 Hz), 7.03 (d, 1H, J = 9.2 Hz), 3.80 (s, 3H), 3.20 (s, 3H). ESI-MS: m/z = 434 $[M+1]^+$.

4.1.13.20. *N*-(2-(1*H*-Indazol-3-yl)-1*H*-pyrrolo[3,2-b]pyridin-5-yl)-3,4-dimethoxy-*N*-methylbenzenesulfonamide (2t). Yellow solid (40%), mp: 88-90 °C. ^{1}H NMR (500 MHz, DMSO-d_6) δ 13.50 (s, 1H), 11.96 (s, 1H), 8.21 (d, 1H, J = 8.0 Hz), 7.83 (d, 1H, J = 8.4 Hz), 7.61 (d, 1H, J = 8.4 Hz), 7.43 (t, 1H, J = 7.6 Hz), 7.33 (d, 1H, J = 8.0 Hz), 7.23 (t, 1H, J = 7.6 Hz), 7.19 (dd, 1H, J = 2.4 Hz, 8.8 Hz), 7.18 (d, 1H, J = 1.2 Hz), 7.07 (d, 1H, J = 8.8 Hz), 6.85 (d, 1H, J = 1.2 Hz), 3.81 (s, 3H), 3.55 (s, 3H), 3.19 (s, 3H). ESI-MS: m/z = 464 $[M+1]^+$.

4.1.13.21. *N*-(2-(1*H*-Indazol-3-yl)-1*H*-pyrrolo[3,2-b]pyridin-5-yl)-2,5-dimethoxy-*N*-methylbenzenesulfonamide (2u). Yellow solid (30%), mp: 90-92 °C. ^{1}H NMR (500 MHz, DMSO-d_6) δ 13.47 (s, 1H), 11.86 (s, 1H), 8.22 (d, 1H, *J* = 8.0 Hz), 7.73 (d, 1H, *J* = 8.4 Hz), 7.61 (d, 1H, *J* = 8.0 Hz), 7.42 (t, 1H, *J* =7.2 Hz), 7.32 (d, 1H, *J* = 2.8 Hz), 7.23 (t, 1H, *J* = 7.2 Hz), 7.22 (d, 1H, *J* = 8.8 Hz), 7.17 (s, 1H), 7.15 (d, 1H, *J* = 2.8 Hz), 7.07 (d, 1H, *J* = 9.2 Hz), 3.74 (s, 3H), 3.48 (s, 3H), 3.37 (s, 3H). ESI-MS: m/z = 464 $[M+1]^+$.

4.1.13.22. *N*-(2-(1*H*-Indazol-3-yl)-1*H*-pyrrolo[3,2-b]pyridin-5-yl)-2,4-dimethoxy-*N*-methylbenzenesulfonamide (2v). Yellow solid (60%), mp: 81-83 °C. ^{1}H NMR (500 MHz, DMSO-d_6) δ 13.46 (s, 1H), 11.82 (s, 1H), 8.22 (d, 1H, *J* = 8.4 Hz), 7.69 (t, 2H, *J* = 8.4 Hz), 7.61 (d, 1H, *J* = 8.4 Hz), 7.42 (t, 1H, *J* = 7.2 Hz), 7.23 (m, 2H), 7.17 (d, 1H, *J* = 1.2 Hz), 6.58 (m, 2H), 3.80 (s, 3H), 3.47 (s, 3H), 3.32 (s, 3H). ESI-MS: m/z = 464 $[M+1]^+$.

4.1.13.23. *N*-(2-(1*H*-Indazol-3-yl)-1*H*-pyrrolo[3,2-b]pyridin-5-yl)-*N*-methyl-3-nitrobenzenesulfonamide (2w). Yellow solid (37%), mp: 92-94 °C. ^{1}H NMR (500 MHz, DMSO-d_6) δ 13.52 (s, 1H), 12.03 (s, 1H), 8.51 (dd, 1H, *J* = 2.4 Hz, 8.4 Hz), 8.34 (s, 1H), 8.18 (d, 1H, *J* = 8.0 Hz), 8.01 (d, 1H, *J* = 7.2 Hz), 7.86 (t, 2H, *J* = 8.0 Hz), 7.62 (d, 1H, *J* = 8.4 Hz), 7.43 (t, 1H, *J* = 8.4 Hz), 7.28 (d, 1H, *J* = 8.8 Hz), 7.24 (t, 1H, *J* = 8.4 Hz), 7.13 (s, 1H), 3.26 (s, 3H). ESI-MS: m/z = 449 $[M+1]^+$.

4.1.13.24. *N*-(2-(1*H*-Indazol-3-yl)-1*H*-pyrrolo[3,2-b]pyridin-5-yl)-*N*-methyl-4-(trifluoromethoxy)-benzenesulfonamide (2x). Yellow solid (45%), mp: 107-109 °C. ^{1}H NMR (500 MHz, DMSO-d_6) δ 10.73 (s, 1H), 9.54 (s, 1H), 8.05 (d, 1H, *J* = 8.5 Hz), 7.67 (m, 3H), 7.53 (d, 1H, *J* = 8.5 Hz), 7.46 (t, 1H, *J* = 7.0 Hz), 7.44 (d, 1H, *J* = 8.5 Hz), 7.29 (t, 1H, *J* = 7.0 Hz), 7.25 (d, 2H, *J* = 8.5 Hz), 7.16 (d, 1H, *J* = 1.0 Hz), 3.36 (s, 3H). ESI-MS: m/z = 488 $[M+1]^+$.

4.1.14. General procedure for the synthesis of 2y and 2z.

Phenyl isocyanate (143 mg, 1.20 mmol) in dry CH_2Cl_2 (3 mL) was added dropwise to **16a** (26.30 mg, 1 mmol) in dry CH_2Cl_2 (5 mL) at room temperature and stirred for 4 h. The reaction was quenched with H_2O (100 mL), extracted with CH_2Cl_2 (10 mL×3) and washed with brine (20 mL×3). The organic layer was dried over anhydrous Na_2SO_4 and concentrated under reduced pressure. The obtained residue was purified by chromatography (petroleum ether/ethanol = 5:1, v/v) to afford **2y** (15 mg).

4.1.14.1. 1-(2-(1*H*-Indazol-3-yl)-1*H*-pyrrolo[3,2-b]pyridin-5-yl)-1-methyl-3-phenylurea (2y). White solid (30%), mp: 217-219 °C. ^{1}H NMR (500 MHz, DMSO-d_6) δ 13.52 (s, 1H), 12.21 (s, 1H), 11.94 (s, 1H), 8.34 (d, 1H, *J* = 10.5 Hz), 7.87 (d, 1H, *J* = 11.0 Hz), 7.64 (m, 3H), 7.46 (t, 1H, *J* = 9.0 Hz), 7.38 (d, 1H, *J* = 1.5 Hz), 7.29 (q, 3H, *J* = 8.0 Hz), 7.11 (d, 1H, *J* = 11.0 Hz), 7.02 (t, 1H, *J* = 9.5 Hz), 3.44 (s, 3H); ^{13}C NMR (125 MHz, DMSO-d_6) δ 153.73, 150.19, 143.00, 141.38, 139.73, 136.85, 135.59, 128.73, 126.63, 126.15, 122.24, 121.61, 121.43, 120.79, 120.05, 119.36, 110.67, 108.32, 99.13, 33.71. ESI-MS: m/z = 383 $[M+1]^+$.

4.1.14.2. 1-(2-(1*H*-Indazol-3-yl)-1*H*-pyrrolo[3,2-b]pyridin-5-yl)-3-(4-methoxyphenyl)-1-methylurea (2z). White solid (34%), mp: 213-215 °C. ^{1}H NMR (500 MHz, DMSO-d_6) δ 11.98 (s, 1H), 11.88 (s, 1H), 10.08 (s, 1H), 8.52 (d, 1H, *J* = 8.0 Hz), 8.41 (d, 1H, *J* = 8.5 Hz), 8.04 (d, 1H, *J* = 9.0 Hz), 7.57 (m, 3H), 7.25 (d, 1H, *J* = 9.0 Hz), 7.05 (d, 2H, *J* = 9.0 Hz), 6.93 (d, 2H, *J* = 9.0 Hz), 3.80 (s, 3H), 3.75 (s, 3H). ESI-MS: m/z = 413 $[M+1]^+$.

4.2. Cell proliferation assay

The antiproliferative activity in vitro was measured using the MTT assay. HL60, KB, SMMC-7721, HCT116, and A549 cell lines were cultured in RPMI-1640 (Invitrogen Corp., Carlsbad, CA) medium with heat-inactivated 10% fetal bovine serum, penicillin (100 units/mL) and streptomycin (100 μg/mL) and incubated in normoxic atmosphere with 20% O_2, 5% CO_2 at 37 ^oC. All tested compounds were dissolved in DMSO at concentrations of 10.0 mg/mL and diluted to appropriate concentrations. Cells were plated in 96-well plates for 24 h and subsequently treated with different concentrations of all tested compounds for 72 h. Viable cells were determined using 3-(4,5-dimethylthiazol-2-yl)-2,5-diphenyltetrazolium bromide assay kit (MTT, Sigma) according to operation instructions provided by the manufacturer. The concentration of drug causing 50% inhibition in absorbance compared with control cells (IC_{50}) was calculated using the software of dose-effect analysis with microcomputers.

4.3. Cell cycle profile (FACS) analysis

HCT116 cells were incubated for 24 h in the presence of compound **2y** (0, 50, 100, 200 nM). Cells were harvested, fixed with 70% ethanol, washed twice with PBS, and stained by 50 μg/mL propidium iodide (PI) solution containing 0.1% Triton X-100, 0.1 mM EDTA, and 50 μg/mL RNase A. Cell cycle was detected by flow cytometry. The cellular DNA content was analyzed by measuring the fluorescence with a FACS Calibur Flow Cytometer (Becton Dickinson Immunocytometry Systems, San Jose, CA).

4.4. Kinase inhibitory assays

For the kinase inhibitory assays, the recombinant Aurora A, GSK3β, and MEK1 proteins were expressed in Escherichia coli system. CDK2/cyclin A was purchased from Carna company. Aurora A, GSK-3β and PKC kinase assays were carried out by using the Z'-LYTE^{TM} Kinase Assay kits (Invitrogen). CDK2/cyclin A, IKKβ kinase assays were carried out by using the HTRF Kinase Assay kits (Cisbio). CHK1 inhibitory activities were determined using the luminescent ADP-Glo assay kit (Promega). Compounds were initially tested at a fixed concentration, and those displaying more than 50% inhibition were further tested for dose-response IC_{50} values. And the results represented an average of at least three experiments.

4.5. Molecular docking

Docking analysis was carried out by using C-DOCKER module (Discovery Studio, version 2.5; Accelrys, San Diego, CA, USA, 2008) to compare the binding modes between compound **2d** bound to Aurora A and **2y** bound to Aurora A. The X-ray crystal structure of Aurora A (PDB ID: 4JAJ) was used for the docking calculation. After removing the ligand and water molecules, the CHARMm-force field was applied to the protein. And the ATP binding pocket was chosen as the active site with a radius set as 8 Å. The ligands were generated random conformations using CHARMm-based molecular dynamics (1000 steps), and then docked into the defined Aurora A binding site. The other parameters were set as default. The final binding conformation of **2d** and **2y** was determined based on the calculated CDOCKING ENERAGE. The most stable binding modes among the top 10 docking poses of **2d** and **2y** were presented in Fig. **3A** and **3B**, respectively.

Acknowledgments

The authors are grateful to the support of the National Natural Science Foundation of China (81172929) and the support of the Program for Zhejiang Leading Team of S&T Innovation (2011R50014). The authors also thank Jianyang Pan (Institute of Pharmaceutical Informatics, Zhejiang University, China) for performing NMR spectrometry and Mass spectrometry for structure elucidation.

Supplementary data

Supplementary data associated with this article can be found, in the online version, at

References

1. (a) de Carcer, G.; Perez de Castro, I.; Malumbres, M., Targeting cell cycle kinases for cancer therapy. *Curr. Med. Chem.* **2007,** *14* (9), 969-985; (b) Tapia-Alveal, C.; Calonge, T. M.; O'Connell, M. J., Regulation of Chk1. *Cell Div.* **2009,** *4* (8).

2. Li, Q.; Zhu, G.-D., Targeting serine/threonine protein kinase B/Akt and cell-cycle checkpoint kinases for treating cancer. *Curr. Top. Med. Chem.* **2002,** *2* (9), 939-971.

3. Lapenna, S.; Giordano, A., Cell cycle kinases as therapeutic targets for cancer. *Nat. Rev. Drug. Discov.* **2009,** *8* (7), 547-566.

4. Alenzi, F. Q. B., Links between apoptosis, proliferation and the cell cycle. *Brit. J. Biomed. Sci.* **2004,** *61* (2), 99-102.

5. (a) Kollareddy, M.; Zheleva, D.; Dzubak, P.; Brahmkshatriya, P. S.; Lepsik, M.; Hajduch, M., Aurora kinase inhibitors: Progress towards the clinic. *Invest. New Drug.* **2012,** *30* (6), 2411-2432; (b) Pitts, T. M.; Davis, S. L.; Eckhardt, S. G.; Bradshaw-Pierce, E. L., Targeting nuclear kinases in cancer: Development of cell cycle kinase inhibitors. *Pharmacol. Ther.* **2014,** *142* (2), 258-269; (c) Maugeri-Sacca, M.; Bartucci, M.; De Maria, R., Checkpoint kinase 1 inhibitors for potentiating systemic anticancer therapy. *Cancer Treat. Rev.* **2013,** *39* (5), 525-533.

6. Fraley, M. E.; Steen, J. T.; Brnardic, E. J.; Arrington, K. L.; Spencer, K. L.; Hanney, B. A.; Kim, Y.; Hartman, G. D.; Stirdivant, S. M.; Drakas, B. A.; Rickert, K.; Walsh, E. S.; Hamilton, K.; Buser, C. A.; Hardwick, J.; Tao, W.; Beck, S. C.; Mao, X.; Lobell, R. B.; Sepp-Lorenzino, L.; Yan, Y.; Ikuta, M.; Munshi, S. K.; Kuo, L. C.; Kreatsoulas, C., 3-(Indol-2-yl)indazoles as Chek1 kinase inhibitors: Optimization of potency and selectivity via substitution at C6. *Bioorg. Med. Chem. Lett.* **2006,** *16* (23), 6049-6053.

7. Dar, A. A.; Goff, L. W.; Majid, S.; Berlin, J.; El-Rifai, W., Aurora Kinase Inhibitors - Rising Stars in Cancer Therapeutics? *Mol. Cancer Ther.* **2010,** *9* (2), 268-278.

8. Katayama, H.; Brinkley, W. R.; Sen, S., The Aurora kinases: role in cell transformation and tumorigenesis. *Cancer Metast. Rev.* **2003,** *22* (4), 451-464.

9. (a) Moore, A. S.; Blagg, J.; Linardopoulos, S.; Pearson, A. D. J., Aurora kinase inhibitors: novel small molecules with promising activity in acute myeloid and Philadelphia-positive leukemias. *Leukemia* **2010,** *24* (4), 671-678; (b) Macarulla, T.; Ramos, F. J.; Tabernero, J., Aurora kinase family: A new target for anticancer drug. *Recent Pat. Anti-Canc.* **2008,** *3* (2), 114-122.

10. Dwyer, M. P.; Paruch, K.; Labroli, M.; Alvarez, C.; Keertikar, K. M.; Poker, C.; Rossman, R.; Fischmann, T. O.; Duca, J. S.; Madison, V.; Parry, D.; Davis, N.; Seghezzi, W.; Wiswell, D.; Guzi, T. J., Discovery of pyrazolo 1,5-a pyrimidine-based CHK1 inhibitors: A template-based approach-Part 1. *Bioorg. Med. Chem. Lett.* **2011,** *21* (1), 467-470.

Figure captions:

Fig. **1** Design of 5-substituted pyrrolopyridin-indazoles as anticancer agents.

Fig. **2** Cell cycle distribution of HCT116 cells after compound **2y** treatment for 24 h. The 2N (diploid) and 4N (tetraploid) DNA content represented the G1 and G2/M phases of the cell cycle, respectively.

Fig. **3** Docking mode comparison between compounds **2d** and **2y** bound to Aurora A. (A) Molecular docking analysis of **2d** with Aurora A. (B) Molecular docking analysis of **2y** with Aurora A. Red dashed lines indicate hydrogen bonds, prepared using PyMOL, PDB ID: 4JAJ.

Scheme **1**. Synthesis of substituted indazole intermediates (**7a**-**c**). Reagents and conditions: (a) $NaNO_2$, $NaBF_4$, KOAc, $CHCl_3$, 53-75%; (b) I_2, KOH, DMF, 47-52%; (c) EtMgBr, Et_2O, $(n\text{-}Bu)_3SnCl$, 45-61%; (d) $(Boc)_2O$, DMAP, THF, 58-68%.

Scheme **2**. Synthesis of 4-azaindole fragment (**14)**. Reagents and conditions: (a) HNO_3, H_2SO_4, 36%; (b) $(Boc)_2O$, DMAP, THF, 87%; (c) NaH, CH_3I, DMF, 58%; (d) DMFDMA, DMF; Pd/C, H_2, MeOH, 69%; (e) $(Boc)_2O$, DMAP, THF, 77%; (f) n-BuLi, I_2, THF, 61%.

Scheme **3**. Synthesis of pyrrolopyridin-indazoles (**2a**-**z**). Reagents and conditions: (a) $Pd(PPh_3)_4$, CuI, toluene, 35-63%; (b) 12 N HCl, EtOH, 39-43%; (c) R_1COCl, Pyridine, 19-77%; (d) R_1SO_2Cl, Pyridine, 25-60%; (e) R_1NCO, CH_2Cl_2, 30-34%.

Table 1. In vitro antiproliferative activities of **2a-n** against five cancer cell lines.

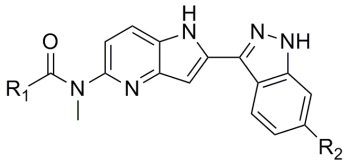

2a-n

Compd	R_1	R_2	Cytotoxicity IC_{50}[a] (μM)				
			HL60	KB	SMMC-7721	HCT116	A549
2a	CH_3-		5.11	10.33	23.38	14.79	>50
2b	CH_3CH_2-		6.13	9.30	33.45	10.75	15.70
2c	$(CH_3)_3C$-		4.99	8.39	22.16	17.98	24.35
2d	Ph-		4.85	8.58	12.53	10.60	13.75
2e	Ph-CH_2-CH_2-		4.73	7.38	20.93	11.23	18.09
2f	4-F-Ph-	H	1.21	7.22	9.15	9.27	9.65
2g	4-Cl-Ph-		0.45	0.63	2.42	3.00	2.22
2h	4-Br-Ph-		1.08	1.78	3.46	6.11	4.25
2i	4-CH_3O-Ph-		3.32	12.90	23.68	29.47	14.56
2j	3-CH_3O-Ph-		1.42	9.01	22.00	14.24	14.87
2k	4-NO_2-Ph-		6.80	20.15	18.42	19.90	34.47
2l	furan-2-yl		4.54	19.43	28.16	29.99	15.49
2m	Ph-	Cl	5.62	5.59	11.27	13.14	9.59
2n	Ph-	CN	6.43	20.93	>50	24.04	32.83

[a] Values are means of three experiments.

Table **2.** In vitro antiproliferative acitivities of **2o-z** against five cancer cell lines.

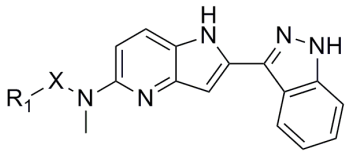

2o-z

Compd	X	R_1	Cytotoxicity IC_{50}[a] (μM)				
			HL60	KB	SMMC-7721	HCT116	A549
2o		Ph-	3.70	2.40	12.00	6.74	14.01
2p		4-CH_3-Ph-	3.03	9.50	16.34	13.33	27.13
2q		4-Cl-Ph-	0.77	8.35	12.68	5.98	18.20
2r		4-Br-Ph-	6.24	7.15	11.53	9.85	19.70
2s	-SO_2-	4-CH_3O-Ph-	4.34	22.12	12.95	22.40	24.25
2t		3,4-di CH_3O-Ph-	6.32	10.05	26.55	16.71	>50
2u		2,5-di CH_3O-Ph-	0.84	4.38	4.28	8.40	19.40
2v		2,4-di CH_3O-Ph-	5.18	10.17	10.77	21.83	25.88
2w		3-NO_2-Ph-	3.66	5.87	5.07	13.58	20.07
2x		4-CF_3O-Ph-	1.17	1.33	7.16	6.04	8.00
2y	-NH-CO-	Ph-	0.0083	0.032	0.28	0.0013	1.43
2z		4-CH_3O-Ph-	0.0079	NT[b]	NT[b]	0.063	NT[b]
Taxol			0.0017	0.015	0.12	0.0049	0.058

[a] Values are means of three experiments.

[b] NT, not tested.

Table **3**. Kinase inhibitory profiles of compounds **2d**, **2g** and **2y**.

Kinases	%Inhibition (1 μg/mL)		
	2d	**2g**	**2y**
CHK1	8.3%	1.0%	20.5%
CDK2	28.23%	35.47%	13.77%
MEK1	3.85%	1.98%	6.64%
GSK3β	18.57%	27.75%	19.26%
BRAF	11.66%	14.37%	16.37%
IKKβ	8.06%	0.94%	0.55%
PKC	5.40%	10.60%	0.62%
Aurora A	95.8% (0.032 μM) [a]	95.0% (0.046 μM) [a]	75.4% (0.519 μM) [a]

[a] Compounds were initially tested at a fixed concentration, those displaying more than 50% inhibition were further tested for dose-response IC_{50} values and the results represented means of at least three experiments.

Scheme 1

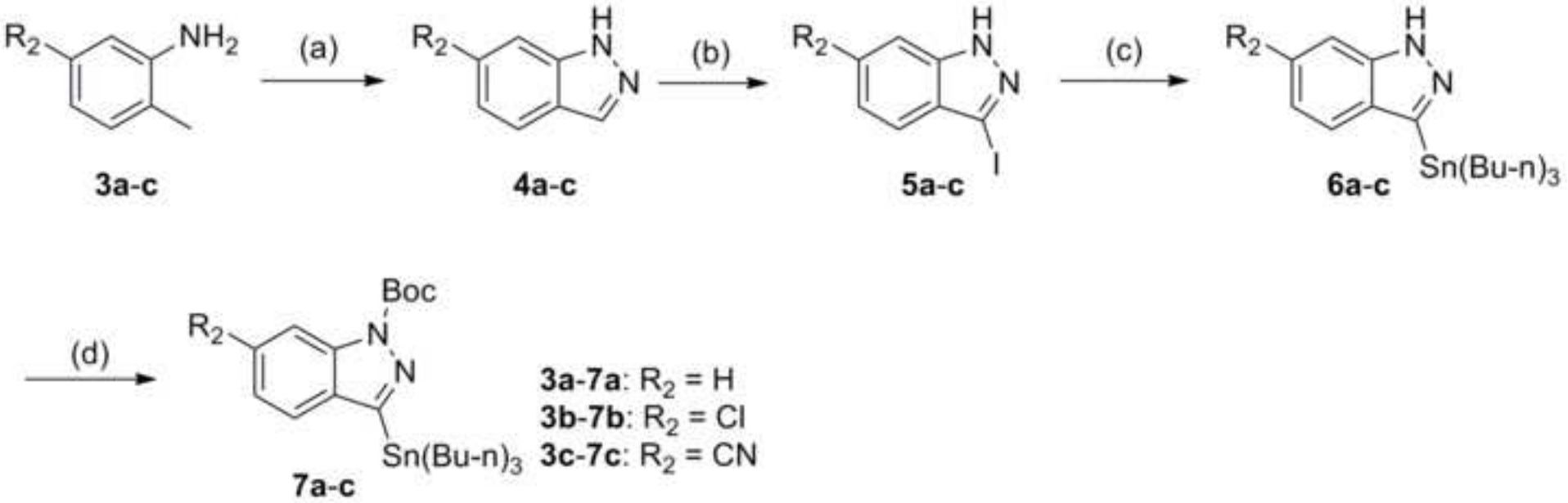

Scheme 2

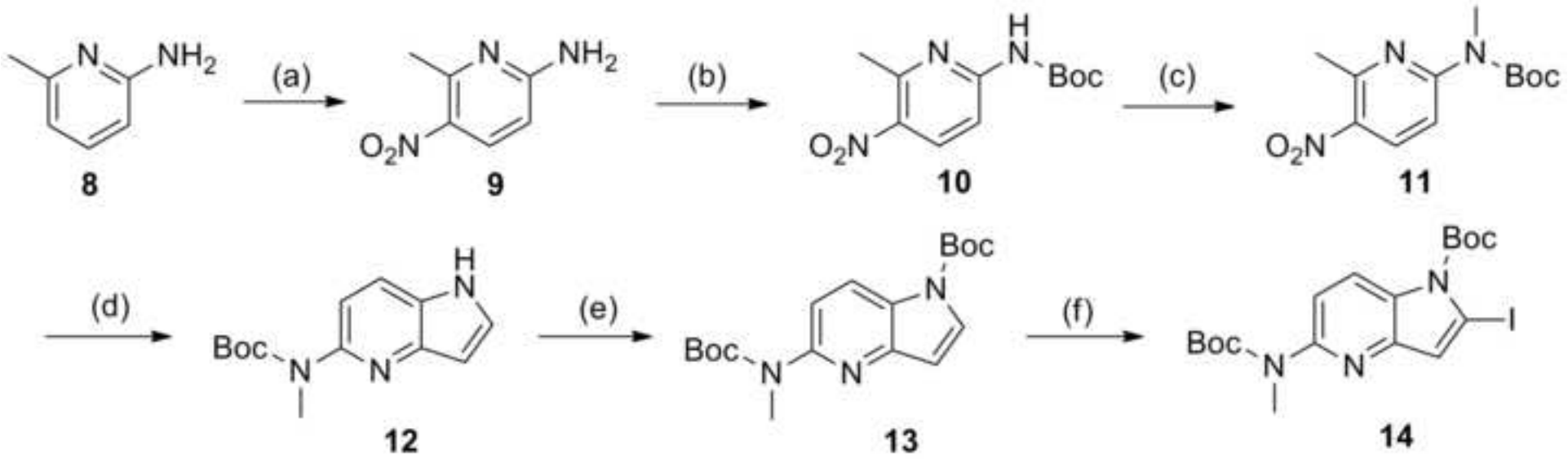

Scheme 3

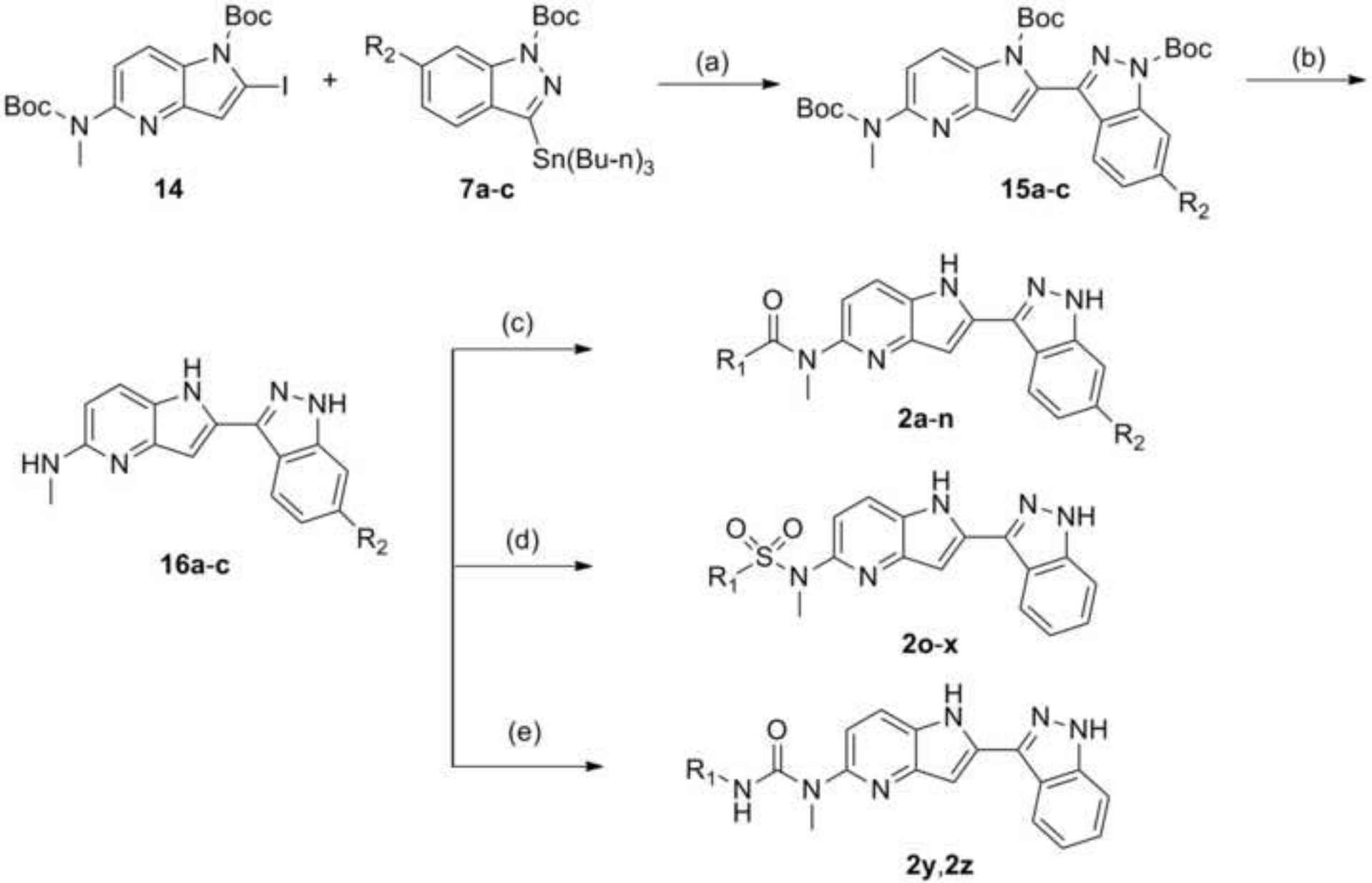

Fig. 1

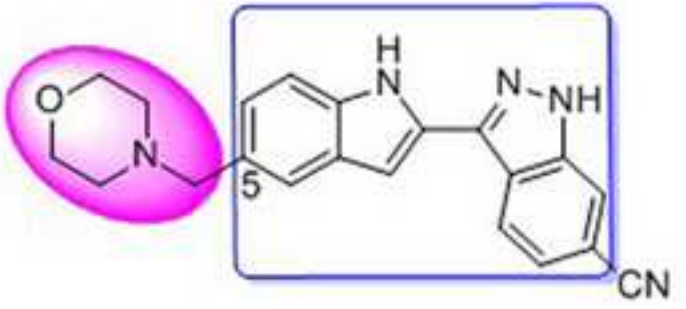

1, CHK1 IC_{50} = 30 nM
CDC7 IC_{50} = 11 nM

R_1 = (hetero)aromatic rings / alkyl groups

R_2 = H / Cl / CN

2a-n

Linker modifications

X = SO_2 / CONH

2o-z

Fig. 2

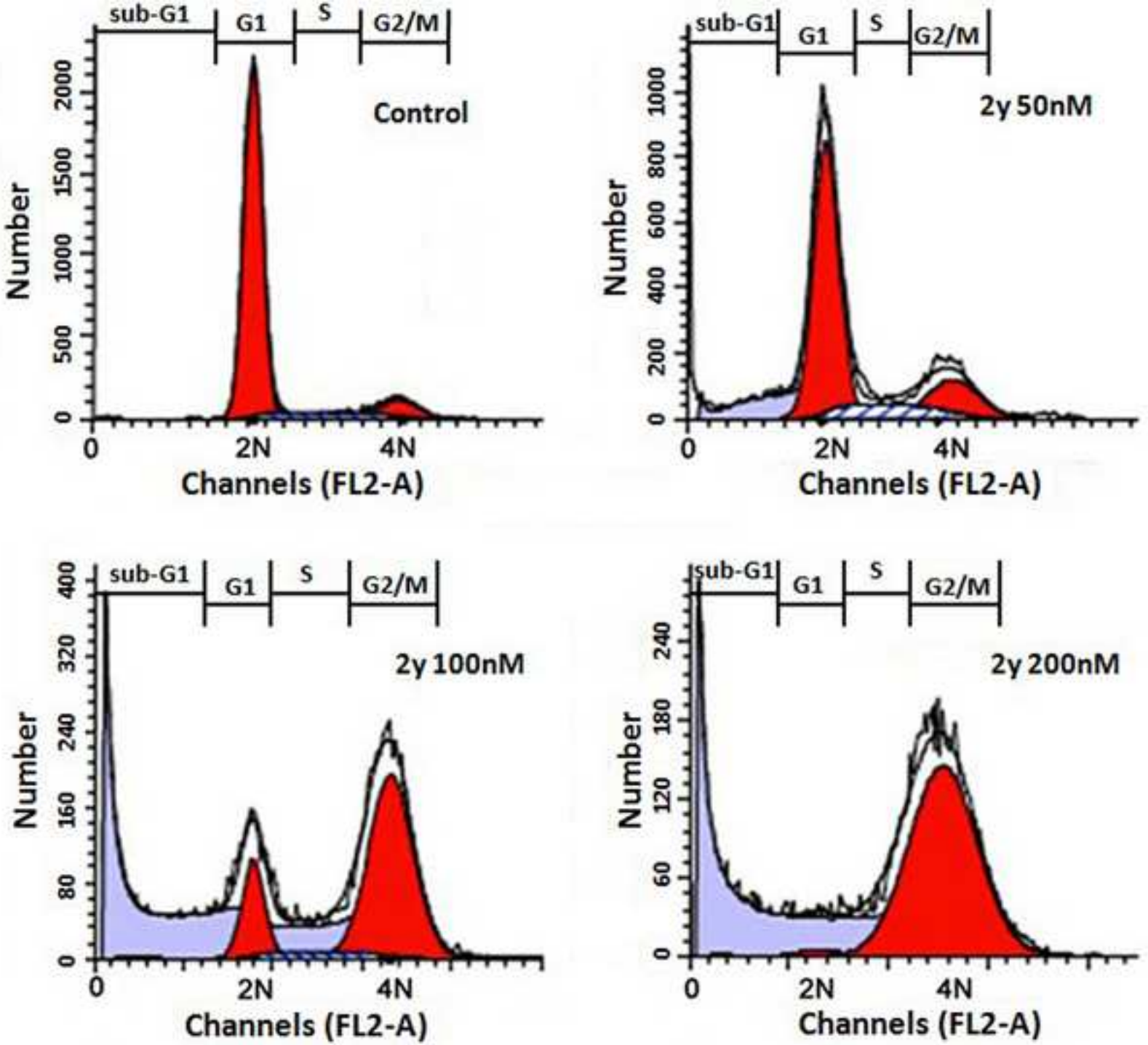

Fig. 3A

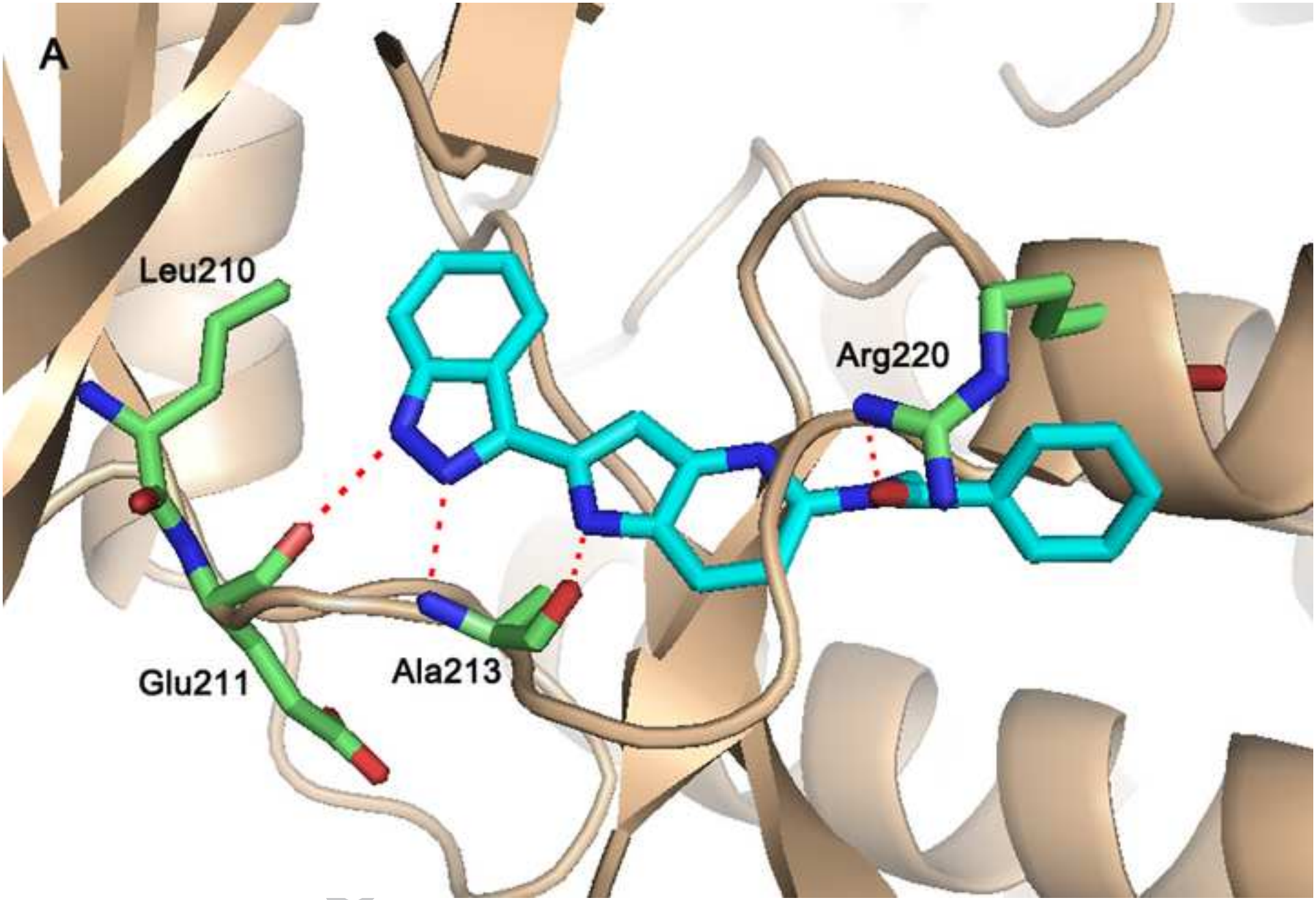

Fig. 3B

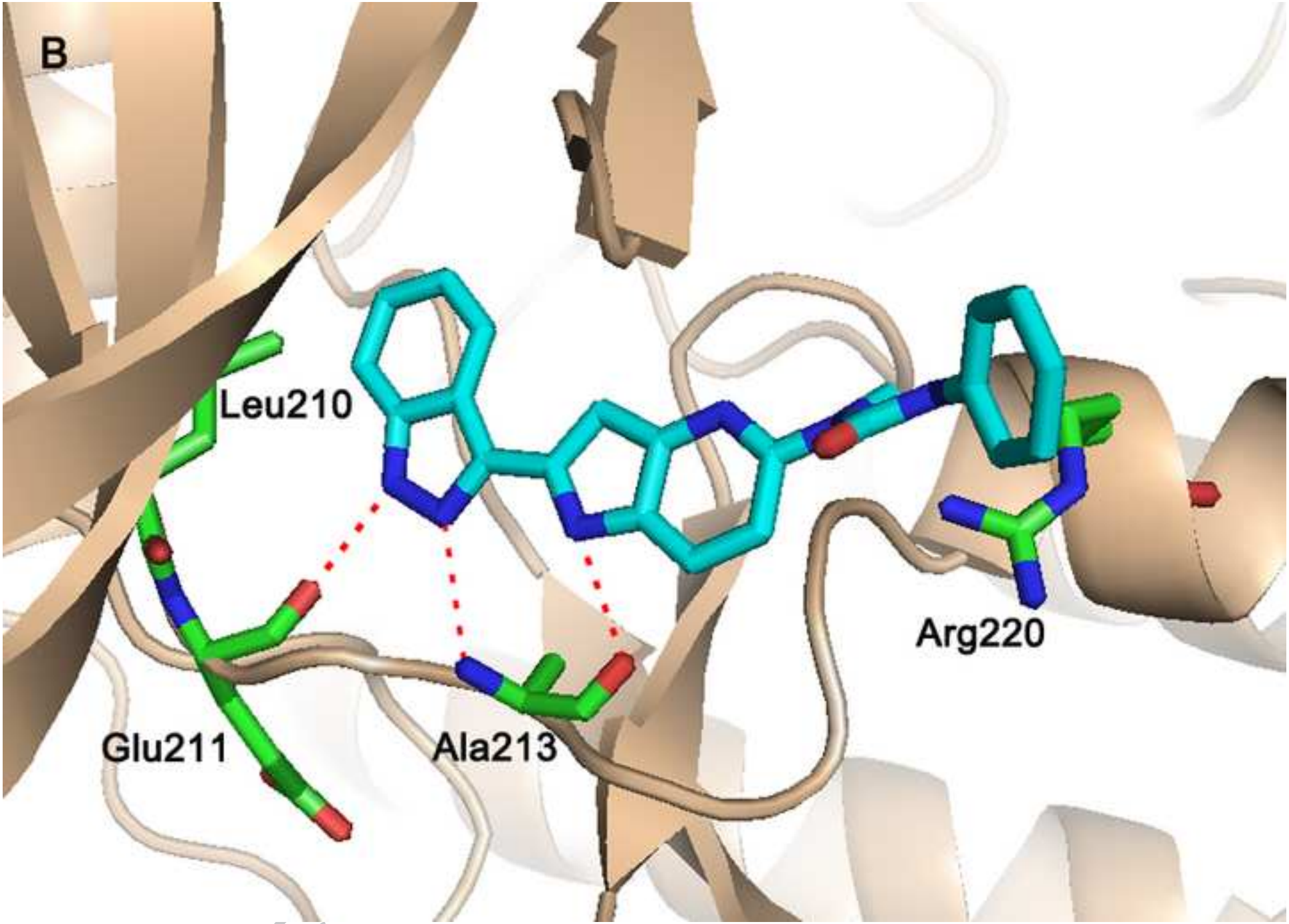

Graphical abstract